2015
ANNUAL REPORT
GEORGIA TECH FUSION RESEARCH CENTER
NUCLEAR & RADIOLOGICAL ENGINEERING PROGRAM
WOODRUFF SCHOOL OF ME, COLLEGE OF ENGINEERING
GEORGIA INSTITUTE OF TECHNOLOGY
July, 2015

PARTICIPANTS: *FACULTY* -- W. M. Stacey; *GRADUATE STUDENT RESEARCHERS*—A. T. Bopp, T. G. Collart, J-P. Floyd, M. Hill, N. Piper, J. Ross, J. J. Rovetto, T. M. Wilks: *UNDERGRADUATE RESEARCHERS*—R. King, S. Mellard, T. Seager; *COLLABORATORS*—T. E. Evans (General Atomics), R. J. Groebner (General Atomics)

RESEARCH ACTIVITIES: I) Collaborative Interpretation of DIII-D Edge Plasma and Rotation Experiments, and **II**) Analysis of Dynamics in SABR Fusion-Fission Hybrid Transmutation Reactor.

I. COLLABORATIVE INTERPRETATION OF DIII-D EDGE PLASMA & ROTATION EXPERIMENTS

"Recent Advances in Plasma Edge Physics Theory; W. M. Stacey *Georgia Tech* This presentation summarizes recent theory developments for interpreting plasma edge physics experiments in DIII-D. i) Radial and poloidal moment balance require that the radial particle flux be of a pinch-diffusive nature with the pinch representing the electromagnetic forces and external momentum input. Ion radial particle fluxes in experiment are found to be a smaller difference between large outward diffusion fluxes and inward pinch fluxes. When the pinch-diffusion relation is used in the continuity equation a new diffusion theory that preserves momentum balance is obtained. ii) The majority of thermalized ions and their energy cross the LCFS on ion loss orbits and are deposited in the SOL near the outboard midplane. The lost ions are predominantly ctr-current, producing a co-current intrinsic rotation of the remaining ions in the edge plasma. iii) While the contribution of the leading order parallel viscosity to toroidal momentum damping vanishes identically in axisymmetric plasmas, non-axisymmetric radial B-fields in the edge plasma enable parallel viscosity to enhance the damping of toroidal rotation. *Work supported by USDoE grant DE-FG01-ER54538

Comparison of Flux-Surface Aligned Curvilinear Coordinate Systems and Neoclassical Magnetic Field Predictions; T. G. Collart and W. M. Stacey, *Georgia Tech*. Several methods are presented for extending the traditional analytic "circular" representation of flux-surface aligned curvilinear coordinate systems to more accurately describe equilibrium plasma geometry and magnetic fields in DIII-D. The formalism originally presented by Miller is extended to include different poloidal variations in the upper and lower hemispheres. A coordinate system based on separate Fourier expansions of major radius and vertical position greatly improves accuracy in edge plasma structure representation. Scale factors and basis vectors for a system formed by expanding the circular model minor radius can be represented using linear combinations of Fourier basis functions. A general method for coordinate system orthogonalization is presented and applied to all curvilinear models. A formalism for the magnetic field structure in these curvilinear models is presented, and the resulting magnetic field predictions are compared against calculations performed in a Cartesian system using an experimentally based EFIT prediction for the Grad-Shafranov equilibrium. *Work supported by USDoE grant DE-FG01-ER54538

"Examination of the Change in Intrinsic Rotation of the DIII-D Edge Pedestal Plasma During the L-H Transition"; N. Piper[1], W.M. Stacey[1], R. j. Groebner[2] 1) *Georgia Tech 2) General Atomics* . A previous analysis of an L-H transition in DIII-D[1] found that the radial particle pinch changed from outward to inward and the co-current edge

intrinsic rotation dropped as the plasma went through the L-H transition. Two additional DIII-D discharges are now being examined in the late L-mode and early H-mode stages to determine if these features are characteristic of the L-H transition. A particle-momentum-energy balance analysis of the measured temperature, density, and rotation velocity is being performed to determine if the particle pinch reverses and the co-current intrinsic rotation due to ion orbit loss drops in the edge pedestal region during the L-H transition. [1]Phys. Plasmas 20, 012509 (2013.

"Determination of the Radial Electric Field in the DIII-D Edge Pedestal Plasma"; T.M. Wilks[1], W.M. Stacey[1], T.E. Evans[2] 1) *Georgia Tech 2) General Atomics* A self-consistent calculation for the radial electric field in the edge plasma for a representative H-mode DIII-D discharge is presented. The complex interrelationships between edge physics phenomena such as rotation, radial ion fluxes, momentum transport, and the radial electric field are maintained by momentum balance requirements. Modeling efforts include fast and thermal ion orbit loss, return currents, x-transport, and a non-axisymmetric rotation formulation, and their effect on radial particle flux, rotation, and the radial electric field. Recent improvements to the non-axisymmetric rotation model demonstrate a new leading order viscosity term contributing further to toroidal rotation damping via non-axisymmetric magnetic fields, which affect the electric field calculation specifically in the edge pedestal region. The new ion orbit loss and rotation model calculations are compared to experiment to show good agreement with the characteristic "well" structure for the radial electric fields in H-mode plasmas. *Work supported by USDoE grant DE-FG01-ER54538

"Comparison of Experimental and Theoretical Thermal Diffusivities in the DIII-D Edge Plasma"; J.J. Roveto, W.M. Stacey, T.M. Wilks; *Georgia Tech* The capability of the Georgia Tech GTEDGE edge transport interpretation code has been upgraded to include improved ion-orbit-loss models for neutral beam and thermalized ions in the edge plasma[1]. We are undertaking a new comparison of various theoretical thermal diffusivity models with the improved interpretation of experimental edge transport now possible. The initial effort is examining two DIII-D shots, #123302, a reference ELMing H-mode shot, and #123301, a matched RMP shot. The improved interpretation leads to quite different experimental thermal diffusivity profiles in the edge than previously reported when ion-orbit-loss effects are included. The experimental values are being compared with various theoretical models, including paleoclassical, neoclassical, ITG, drift ballooning mode, TEM, and ETG. [1] T. M. Wilkes et al., Transport Task Force 2015.

"Evolution of edge pedestal transport between ELMs in DIII-D", J-P. Floyd[1], W. M. Stacey[1], R. J. Groebner[2], and S. C. Mellard[1] , *[1]Georgia Tech, [2]General Atomics*. Evolution of measured profiles of densities, temperatures and velocities in the edge pedestal region between successive ELM (edge-localized mode) events are analyzed and interpreted in terms of the constraints imposed by particle, momentum and energy balance in order to gain insights regarding the underlying evolution of transport processes in the edge pedestal between ELMs in a series of DIII-D discharges. The data from successive inter-ELM periods during an otherwise steady-state phase of the discharges were combined into a composite inter-ELM period for the purpose of increasing the number of data points in the analysis. Variation of diffusive and non-diffusive (pinch) particle, momentum, and energy transport over the inter-ELM period are interpreted using the GTEDGE code for discharges with plasma currents from 0.5 to 1.5 MA and inter-ELM periods from 50 to 220 ms. Diffusive transport is dominant for $\rho < 0.925$, while non-diffusive and diffusive transport are very large and nearly balancing in the sharp gradient region $0.925 < \rho < 1.0$. During the inter-ELM period, diffusive transport increases slightly more than non-diffusive transport, increasing net outward transport. Both diffusive and non-diffusive transport have a strong inverse correlation with plasma current. *Work supported by USDoE grant DE-FG01-ER54538

II. ANALYSIS OF DYNAMICS IN ITER AND SABR FUSION-FISSION HYBRID TRANSMUTATION REACTOR

"Burn Control Mechanisms in Tokamaks,* M. Hill and W. M. Stacey, *Georgia Tech.* Burn control and passive safety in accident scenarios will be an important design consideration in future tokamak reactors, in particular fusion-fission hybrid reactors, e.g. the Subcritical Advanced Burner Reactor. We are developing a burning plasma dynamics code to explore various aspects of burn control, with the intent to identify feedback mechanisms that would prevent power excursions. This code solves the coupled set of global density and temperature equations, using scaling relations from experimental fits. Predictions of densities and temperatures have been benchmarked against DIII-D data. We are examining several potential feedback mechanisms to limit power excursions: i) ion-orbit loss, ii) thermal instability density limits, iii) MHD instability limits, iv) the degradation of alpha-particle confinement, v) modifications to the radial current profile, vi) "divertor choking" and vii) Type 1 ELMs.

A Nodal Kinetics Model for a Fission-Fusion Hybrid Reactor

A. T. Bopp, W. M. Stacey

Fast Reactor Research Group, Georgia Institute of Technology, 770 State St, Atlanta, GA 30332
abopp3@gatech.edu

INTRODUCTION

The Subcritical Advanced Burner Reactor (SABR) [1] is an amalgam of an ITER-like fusion neutron source [2] and a modular, IFR-like [3], sodium cooled, metal fueled, pool type fast reactor. The IFR's design (and consequently SABR's design), is based on EBR-II [4]. EBR-II was demonstrated to be inherently safe [5], and the purpose of our work is to determine if SABR retains this important feature. SABR is composed of 10 physically separate but neutronically coupled cores each within a separate sodium pool. During any type of transient or perturbation, spatial flux tilts could become an issue. Thus, we are developing a dynamics model that relies on a nodal kinetics approach instead of the more traditional point kinetics approach.

NODAL KINETICS EQUATIONS

$$\frac{dn_j(t)}{dt} = \frac{(1-\beta_j)}{\Lambda_j} n_j(t) + \sum_{i=1}^{6} (\lambda_{i,j} c_{i,j}) + \frac{n_j(t)}{\tau_j} + S_{fus} + \sum_{k=1}^{10} \frac{\alpha_{kj} n_k(t)}{l_{e,k}} - \frac{n_j(t)}{l_{e,j}} - \frac{n_j(t)}{l_{a,j}} \quad (1)$$

$$\frac{dc_{i,j}(t)}{dt} = \frac{\beta_{i,j}}{\Lambda_j} n_j(t) - \lambda_{i,j} c_{i,j} \quad (2)$$

$$\Lambda_j = \frac{1}{V \nu \Sigma_{f,j}} \quad , \quad \tau_j = \frac{1}{V 2\Sigma_{n2n,j}} \quad (3)$$

The nodal kinetics equations for SABR are shown in Eq. (1) and Eq. (2). The resulting 70 coupled differential equations can be solved numerically. The terms in Eq. (1) are conventional nodal kinetics terms with only a few exceptions. $n_j(t)$ is the neutron density of node j. β_j is the delayed neutron fraction. $c_{i,j}$ and $\lambda_{i,j}$ represent the six groups of delayed neutron precursor densities and their respective half-lives. Eq. (3) defines the fission generation time Λ_j and the n,2n generation time τ_j. n,2n reactions are a non-neglible source in the system and must be accounted for due to the hard neutron spectrum. $l_{e,j}$ and $l_{a,j}$ are the neutron escape and absorption lifetimes respectively. The contribution of neutrons from the fusion plasma is represented by the term S_{fus}. The neutronic coupling is represented by a node k to node j coupling coefficient α_{kj}, which is the probability that a neutron emitted from the surface of node k will impinge upon the surface of node j before entering any other nodes. The rate of neutrons entering node j from node k is α_{kj} times the rate at which neutrons are escaping from node k. The coupling coefficients along with all of the other kinetics parameters used in the above equations are calculated using MCNP6 [6]. The MCNP model

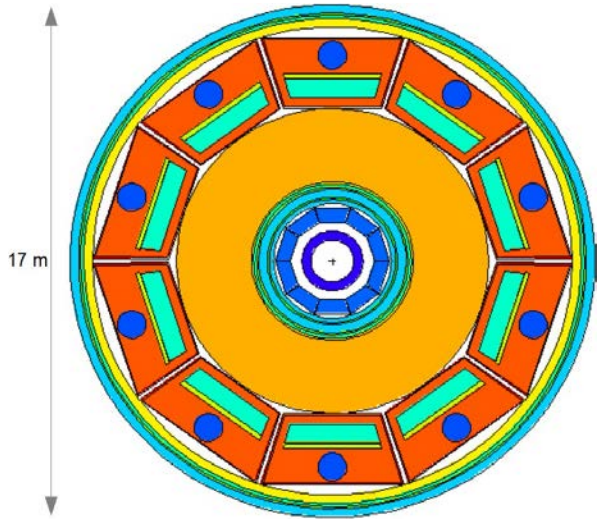

Fig. 1. R-θ view of SABR MCNP model.

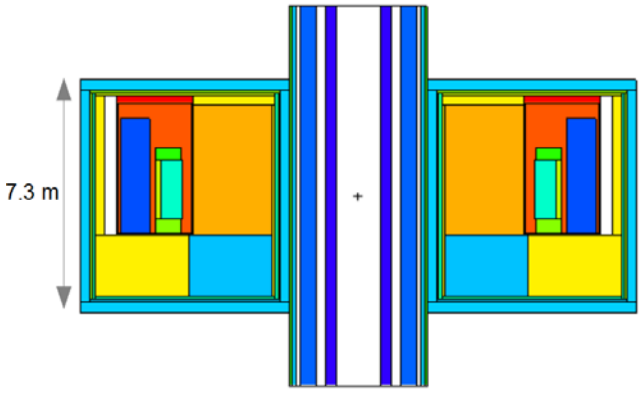

Fig. 2. R-Z view of SABR MCNP model.

is an approximated 3D representation of SABR. A kinetics node is defined as the active fuel region of each core. A node does not include any of the upper or lower internals of the fuel assemblies. An R-θ top-down view, and a R-Z side view of the MCNP model can be seen in Figure 1 and Figure 2.

MODEL VERIFICATION

$$k_{eff} = \frac{\sum_{j=1}^{10} \left(\frac{n_j V_j}{\Lambda_j}\right)}{\sum_{j=1}^{10} \left(\frac{n_j V_j}{l_{e,j}} + \frac{n_j V_j}{l_{a,j}} - \frac{n_j V_j}{\tau_j} - \sum_{k=1}^{10} \left(\frac{\alpha_{kj} n_k V_k}{l_{e,k}}\right)\right)} \quad (4)$$

If the terms in Eq. (1) represent an accurate neutron bal-

ance and its terms are calculated correctly in MCNP, then the k_{eff} predicted by Eq. (4) will closely match the k_{eff} calculated by a KCODE run in MCNP. KCODE calculates k_{eff} = 0.97392 ± 0.00008 while the nodal based estimate of Eq. (4) calculates k_{eff} = 0.97428. Future tests will check the accuracy of the fusion neutron source representation and examine the time dependence of other kinetics terms.

FUTURE WORK

Once the nodal kinetics model is well-developed, the next step is building a reactivity model that will calculate a variety feedback coefficients. Using that information, Eq. (1) and Eq. (2) can be solved numerically. The end goal of this work is to perform a dynamic safety analysis of SABR. This will be done by building a model of SABR's heat removal system in COMSOL that is coupled to the kinetics solver. For every time step in the transient, COMSOL will first solve all of the fluid and thermal equations and then send the temperature profiles to the kinetics solver. The kinetics solver will convert the temperatures to changes in kinetics parameters and then the changes in power. The dynamics of the plasma neutron source will be modeled separately and coupled to the COMSOL model. The end result will be a dynamic safety model that can incorporate the interesting physics of a fission-fusion hybrid burner reactor.

REFERENCES

1. W. M. STACEY ET AL., "Resolution of Fission and Fusion Technology Integration Issues: An Upgraded Design Concept for the Subcritical Advanced Burner Reactor," *Nuclear Technology*, **187**, 15–43 (2014).
2. "ITER Website," www.iter.org.
3. C. E. TILL and Y. I. CHANG, *Plentiful Energy: The Story of the Integral Fast Reactor: The complex history of a simple reactor technology, with emphasis on its scientific bases for non-specialists*, CreateSpace Independent Publishing Platform (2011).
4. C. WESTFALL, "Vision and reality: The EBR-II story," *Nuclear News*, pp. 25–32 (February 2004).
5. H. P. PLANCHON ET AL., "Results and Implications of the Experimental Breeder Reactor II Inherent Safety Demonstration Tests," *Nuclear Science and Engineering*, **100**, 549–557 (1988).
6. "MCNP Website," https://mcnp.lanl.gov/.